HHS Public Access

Author manuscript

Nat Struct Mol Biol. Author manuscript; available in PMC 2017 July 09.

Published in final edited form as:

Nat Struct Mol Biol. 2017 February ; 24(2): 184–186. doi:10.1038/nsmb.3352.

Structure of the immature Zika virus at 9 Å resolution

Vidya Mangala Prasad, **Andrew S. Miller**, **Thomas Klose**, **Devika Sirohi**, **Geeta Buda**, **Wen Jiang**, **Richard J. Kuhn**, and **Michael G. Rossmann**

Department of Biological Sciences, Purdue University, West Lafayette, Indiana 47907, USA

Abstract

The current Zika virus (ZIKV) epidemic is characterized by severe pathogenicity in both children and adults. Sequence changes in ZIKV since its first isolation, are apparent when comparing “pre-epidemic” strains with those causing the current epidemic. However, the residues that are responsible for ZIKV pathogenicity are largely unknown. Here, we report the cryo-electron microscopy (cryo-EM) structure of the immature ZIKV at 9 Å resolution. The cryo-EM map was fitted with the crystal structures of the precursor membrane and envelope glycoproteins and was shown to be similar to the structures of other known immature flaviviruses. However, the immature ZIKV contains a partially ordered capsid protein shell that is less prominent in other immature flaviviruses. Furthermore, six amino acids near the interface between pr domains at the top of the spikes were found to be different between the “pre-epidemic” and “epidemic” ZIKV, possibly influencing the composition and structure of the resulting viruses.

The current Zika virus (ZIKV) epidemic, which started in Brazil in 2015, has given rise to reports of microcephaly in fetuses[1] and Guillian Barre syndrome[2] in adults. ZIKV is a member of the *Flaviviridae* family and, like some other flaviviruses, is transmitted by mosquitos. The flaviviruses include other significant human pathogens such as dengue virus (DENV), West Nile virus (WNV), yellow fever virus (YFV) and Japanese encephalitis virus (JEV)[3]. Flaviviruses are enveloped viruses containing a single-stranded, positive-sense, RNA genome of ~11kb (ref. 3). The RNA genome is complexed with multiple capsid protein molecules, surrounded by a membrane, in virions[4]. The extracellular, mature form of the virus has an outer surface that forms an icosahedral shell with 90 dimers of the envelope (E) (~495 amino acids) and the membrane (M) (~75 amino acids) proteins, arranged in a

Correspondence should be addressed to M.G.R., Department of Biological Sciences, 240 S. Martin Jischke Drive, Purdue University, West Lafayette, Indiana 47907, USA; telephone: (765) 494-4911; mr@purdue.edu or R.J.K., Department of Biological Sciences, 240 S. Martin Jischke Drive, Purdue University, West Lafayette, Indiana 47907, USA; telephone: (765) 494-8149; kuhnr@purdue.edu.

AUTHOR CONTRIBUTIONS

A.M, D.S and G.B were involved in preparation of cell culture, optimization and purification of virus sample. V.M.P. and T.K conducted the cryo-EM preparation, data collection and data processing; V.M.P. performed the data analyses; W.J. made his *jspr* program available for reconstruction and refinement of the cryo-EM map. V.M.P., R.J.K and M.G.R. wrote the paper.

COMPETING FINANCIAL INTERESTS

The authors declare no competing financial interests.

Accession Codes/Data availability. The atomic coordinates of the fitted dengue virus-2 prM-E molecules and mature ZIKV E and M transmembrane components along with the cryo-EM density map of the immature ZIKV are available at the Protein Data Bank and Electron Microscopy Data Bank with accession codes 5U4W and EMD-8508, respectively.

"herring-bone" pattern[5]. The E glycoprotein is involved in receptor binding, attachment and virus fusion during cell entry[4]. The M protein is mostly unexposed and has a significant transmembrane component. The cryo-EM structures of different, mature flaviviruses[5–7] including ZIKV[8, 9] are known and have a similar overall architecture (Fig. 1a and b). During infection of host cells, virions first assemble into an immature form of the virus in the endoplasmic recticulum[3]. The immature virus is composed of 60 trimeric spikes of the precursor membrane (prM) and E proteins where the pr domain (~90 amino acids) of the prM protein protects the fusion loop on the E protein from non-productive interactions within the cell[10]. In the low pH environment of the trans-Golgi network, the immature virions undergo proteolytic processing by furin, a cellular protease[11], and the pr domain is cleaved from the prM protein during maturation. The virus then releases the pr domain to form the mature virion on exit from cells[12].

Although only the mature form of the virus is considered infectious; due to varying efficiency of pr cleavage in flaviviruses[3], the virus population secreted from host cells is a mixture of mature, partially mature and immature virions. Immature forms of flaviviruses such as DENV[13] and WNV[14] can become infectious through antibody dependent entry of host cells. ZIKV is no exception to this observation of a mixed population of virus maturation states on release from infected cells. It is, thus, probable that the immature form of ZIKV also plays a role in virus infection and spread.

Here, we report a cryo-EM structure of the immature ZIKV (H/PF/2013 strain of Asian lineage) at a resolution of 9 Å. This structure has been used to fit the crystal structures of the prM and E proteins into the cryo-EM map and compared with immature virion structures from other flaviviruses.

RESULTS

Cryo-EM structure of immature ZIKV

Mosquito C6/36 cells were infected with ZIKV (strain H/PF/2013) for 16hrs at 30°C followed by addition of NH_4Cl to produce immature virions. The purified immature ZIKV was plunge frozen on grids and examined using an FEI Titan Krios electron microscope with a Gatan K2 Summit detector. Although the purified viruses were predominantly spiky, as expected for immature particles, they appeared to have some heterogeneity. A total of 9315 particles were selected and used to generate a cryo-EM map at a resolution of 9.1 Å based on the 0.143 Fourier shell correlation criterion (Supplementary Fig. 1).

The cryo-EM reconstruction of the immature ZIKV has a spiky appearance with a diameter of approximately 600 Å (Fig. 1c and d). Densities for the individual prM-E heterodimers within the spikes are clearly visible in the immature ZIKV cryo-EM map. In addition, the individual transmembrane regions of the E and M proteins are easily recognizable. The crystal structure of the DENV-2 prM-E ectodomain heterodimer (PDB ID: 3C6E)[15] was fitted into the immature ZIKV cryo-EM map at the three independent positions with one trimeric spike (**Methods** and Supplementary Fig. 2a–c). The transmembrane helices of the M and E proteins from the mature ZIKV were also fitted individually into the transmembrane densities in the immature ZIKV cryo-EM map (Supplementary Fig. 2d). A

comparison of these fitted components in ZIKV to the complete trimeric prM-E spike of immature DENV-1 (ref.16) showed little difference in spatial arrangement.

Glycosylation in immature ZIKV

The fitting procedure showed that Asn 69 of the pr domain in ZIKV is glycosylated, as also in DENV (Supplementary Fig. 3a), but the glycosylation at Asn 67 position on the DENV E protein is not preserved in ZIKV (Supplementary Fig. 3b). Additional density was also found associated with each of the three Asn 154 residues in the immature ZIKV (Supplementary Fig. 3c), showing that Asn 154 is glycosylated as expected from the protein sequence. Similarly, Asn 154 on the E protein is glycosylated in the mature ZIKV and was found to cover the fusion loop in the adjacent E monomer, suggesting that this site maybe important for viral entry[8].

Inner shell of capsid protein in immature ZIKV

Residual density is observed between the inner membrane layer and the RNA core (Fig. 1d). The density is immediately below the base of each of the spikes and has a volume and shape that matches that of dimeric capsid protein structure[17, 18] (Fig. 1d and Fig. 2a–d). This potential capsid density is more evident in immature ZIKV than in immature DENV-1 (ref. 16). Mature flavivirus structures[5, 8] lack density in this region (Fig. 1b), suggesting a rearrangement of the capsid shell during maturation. The capsid density is in contact with the inner layer of the viral membrane and is close to the transmembrane domains of the E and M proteins, suggesting interactions that might be essential during virion assembly. The other benefit provided by the formation of an inner shell of capsid proteins is for recruitment of the viral genome. Moreover, the advantage of having a somewhat unstable inner core, as shown here for ZIKV, could be to facilitate transfer of the genome into a host cell during infection.

Interactions between prM-E heterodimers of the trimeric spikes

The three prM-E hetrodimers that form a spike in immature flaviviruses are not related by three-fold symmetry. Thus the interactions of any one of the three heterodimers with the two others in a spike is different. The trimeric spike in immature ZIKV is held together at its external tip through interactions between the pr domains and the fusion loop of one of the E proteins (Fig. 3a and b). The residues involved in these interactions between prM-E heterodimers within the spikes can be deduced from the DENV-2 prM-E crystal structure fitted into the trimeric spike density of ZIKV and the sequence alignment of prM-E for DENV-2 and ZIKV (H/PF/2013) (Fig. 3b, Supplementary Fig. 4 and Supplementary Table 1). Apart from these interactions at the top of the trimeric spikes, the base of the spike is stabilized by interactions between residues in domain III of the ZIKV-E protein in one spike to the domain II of E protein from an adjacent spike (Fig. 3c, Supplementary Fig. 4 and Supplementary Table 1).

Amongst flaviviruses, the prM protein has the lowest percentage identity (~40%) when compared to the other viral proteins. Even when comparing between different strains of ZIKV, the pr domain has the highest percentage of changes in its amino acid sequence compared to other ZIKV proteins[19]. There are six amino acid changes in the pr domain

between pre-epidemic and epidemic ZIKV strains and all of these are contained in the ~40 amino acids at the start of the pr domain[19] (Fig. 3). These amino acid changes cluster near the interface between pr domains which are involved in the interactions within trimeric spikes (Fig. 3b and Supplementary Fig. 4). A few of these amino acid substitutions involve dramatic changes in the polarity of the residues, for example, Lys-21 and His-35 in pre-epidemic ZIKV strains are substituted by Glu-21 and Tyr-35 in the epidemic strains. Similarly, change in Val-26 to Pro-26 between the pre-epidemic to epidemic ZIKV strains can potentially affect the local Cα backbone structure in the pr domain. Thus, these amino acid changes possess the ability to alter the nature of interactions within a trimer spike among the different strains of ZIKV.

DISCUSSION

Comparison between the residues near the interface within trimeric spikes in DENV to that in the epidemic ZIKV strains shows that the interface in DENV is more positively charged than in ZIKV (Supplementary Fig. 4). Lack of such closely positioned positively charged residues in ZIKV could imply comparatively more stable interactions within spikes in immature ZIKV. This would have an effect on the dynamics of conformational change between the immature and mature virion states, wherein the trimeric spikes have to break contacts to form the dimeric interactions seen in mature virions. Thus, ZIKV may have a tendency to have a higher proportion of partially immature virions in their populations than completely mature virions. This partial maturation of virions is seen in all flaviviruses, but the degree of heterogeneity of virion particles varies between flaviviruses[3]. A structurally heterogeneous virion population is advantageous to a viral pathogen, as it limits the uniform availability of neutralizing epitopes on the virion, making it more challenging for the host immune system to inhibit the virus. This phenomenon is not only observed with other flaviviruses, such as WNV[20, 21], but also for other debilitating viruses such as HIV-1 (refs. 22, 23). In addition, non-neutralizing antibody responses can be counteractively used by ZIKV for antibody-dependent entry of host cells[24, 25]. Thus, local differences between ZIKV strains, could modulate the sensitivity of ZIKV to antibodies and impact the potency of viral infection.

ONLINE METHODS

Virus preparation and purification

Approximately 1×10^9 C6/36 cells (ATCC CRL-1660) were infected with Zika virus (strain H/PF/2013) at a multiplicity of infection of 4 for 16hrs at 30°C. The inoculum was removed and cells were rinsed three times with phosphate buffered saline (pH 8.0) and incubated for two hours at 30°C in minimal essential media containing 2% fetal bovine serum, 25mM HEPES pH 7.3, and 30mM NH_4Cl. The process was repeated two more times for a total of three incubations at 30°C in cell culture media containing 30mM NH_4Cl. Media was collected 72 hours post infection and immature virus particles were purified according to previously described methods[12]. Briefly, virus particles were precipitated from the media by overnight mixing with 8% polyethylene glycol 8000 at 4°C. This mixture was then pelleted at 8900×*g* for 50 minutes at 4°C. Resuspended particles were pelleted through a 24%

sucrose cushion, resuspended in 0.5mL NTE buffer (20mM Tris pH 8.0, 120mM NaCl, 1mM EDTA) and purified with a discontinuous gradient in 5% intervals from 35% to 10% K-tartrate, 20mM Tris pH 8.0 and 1mM EDTA. Immature virus was extracted from the gradient, concentrated and buffer exchanged into NTE buffer.

Cryo-electron microscopy data collection

The purified immature ZIKV sample was plunge frozen on ultrathin lacey carbon EM grids (Electron Microscopy Sciences). The grids were examined using an FEI Titan Krios electron microscope with a Gatan K2 Summit detector. Cryo-EM images were collected at a magnification of 22,500× in the "super-resolution" data collection mode. The pixel size of the collected images was 0.65 Å. The total exposure time for producing one image composed of 38 frames was 7.6 s and required a dose rate of 4.7 electrons $Å^{-2}$ s^{-1}. A total of 3341 images were collected and 14351 particles were boxed manually using the e2boxer program from the EMAN2 software[26].

Three-dimensional reconstruction and data analysis

Non-reference two-dimensional classification was performed using the Relion software package[27] resulting in the selection of 9315 particles. This dataset was split into two equal subsets as required by the "gold standard" for determining the quality of the cryo-EM reconstruction. The *jspr* program[28] was used for initial model generation and refinement of the orientations of the selected particles. The selected particles were used to generate a cryo-EM map at an average resolution of 9.34 Å based on the 0.143 Fourier shell correlation criterion. After the application of soft spherical masks, the resolution improved to 9.14 Å.

Fitting of crystal structures into the cryo-EM map

The crystal structure of immature dengue virus-2 prM-E heterodimer (PDB ID: 3C6E) was used for fitting into a trimeric spike in the immature ZIKV map. Sequential fitting of the three prM-E molecules into the trimeric spike density was carried out using the UCSF Chimera software[29]. The Cα backbone of the transmembrane helices of M and E proteins from the mature ZIKV structure (PDB ID: 5IRE) were also fitted into the transmembrane regions of the three prM-E heterodimers. The solution structure of DENV-2 capsid protein (PDB ID: 1R6R) was placed into the density between the inner layer of the viral membrane and the RNA core of immature ZIKV, according to previously suggested orientation of the capsid protein in the virion[17]. The mature ZIKV E protein's ectodomain structure (PDB ID: 5IRE)[8] was split into two parts, with one molecule containing the domain I plus III and the second molecule containing domain II. These different parts were superposed independently on the immature dengue prM-E molecule for determining the interaction regions between E proteins from adjacent spikes. Interface regions between different protein partners were identified as residues with less than 6 Å distance between their corresponding Cα backbones.

Multiple sequence alignment

Sequence alignments of the pr domain and E glycoprotein amongst flaviviruses were carried out using the MAFFT program[30] and rendered using the ESPript software[31]. The sequences

for comparison were obtained from the ViPR resource database[32]. The representative flavivirus strains used in the comparison were Zika-Asian (H/PF/2013 strain), Zika-African (1968-Nigeria strain), West Nile virus (NY99 strain), Japanese encephalitis virus (SA14), yellow fever virus (Asibi strain) and the four dengue virus serotypes (Western Pacific, S16803, CH53489 and IND1979 strains). In the manuscript, the residue numbers for pr and E are used based on the ZIKV sequence and structure, though the numbers assigned to the residues during multiple sequence alignment may have slightly shifted in Supplementary Fig. 4.

Supplementary Material

Refer to Web version on PubMed Central for supplementary material.

Acknowledgments

We thank Dr. Madhumati Sevvana for helpful discussions about the manuscript. We thank Sheryl Kelly for help in preparation of the manuscript. We also thank the Purdue Cryo-EM Facility for equipment access and support. This work was supported by the National Institutes of Health (RO1 AI076331 awarded to M.G.R and R.J.K and a sub-award for RO1 AI073755 (P.I: M. S. Diamond, Washington University) to both M.G.R and R.J.K.).

REFERENCES

1. Schuler-Faccini L, et al. Possible association between Zika virus infection and microcephaly - Brazil, 2015. MMWR Morb. Mortal. Wkly. Rep. 2016; 65:59–62. [PubMed: 26820244]
2. Chan JF, Choi GK, Yip CC, Cheng VC, Yuen KY. Zika fever and congenital Zika syndrome: An unexpected emerging arboviral disease. J. Infect. 2016; 72:507–524. [PubMed: 26940504]
3. Lindenbach, BD., Murray, CL., Thiel, H-J., Rice, CM. *Flaviviridae*: The viruses and their replication. In: Knipe, DM., et al., editors. Fields Virology. Lippincott Williams & Wilkins; 2013.
4. Mukhopadhyay S, Kuhn RJ, Rossmann MG. A structural perspective of the flavivirus life cycle. Nat. Rev. Microbiol. 2005; 3:13–22. [PubMed: 15608696]
5. Kuhn RJ, et al. Structure of dengue virus: implications for flavivirus organization, maturation, and fusion. Cell. 2002; 108:717–725. [PubMed: 11893341]
6. Mukhopadhyay S, Kim BS, Chipman PR, Rossmann MG, Kuhn RJ. Structure of West Nile virus. Science. 2003; 302:248. [PubMed: 14551429]
7. Zhang X, et al. Cryo-EM structure of the mature dengue virus at 3.5-Å resolution. Nat. Struct. Mol. Biol. 2013; 20:105–110. [PubMed: 23241927]
8. Sirohi D, et al. The 3.8 Å resolution cryo-EM structure of Zika virus. Science. 2016; 352:467–470. [PubMed: 27033547]
9. Kostyuchenko VA, et al. Structure of the thermally stable Zika virus. Nature. 2016; 533:425–428. [PubMed: 27093288]
10. Zhang Y, et al. Structures of immature flavivirus particles. EMBO J. 2003; 22:2604–2613. [PubMed: 12773377]
11. Stadler K, Allison SL, Schalich J, Heinz FX. Proteolytic activation of tick-borne encephalitis virus by furin. J. Virol. 1997; 71:8475–8481. [PubMed: 9343204]
12. Yu I-M, et al. Structure of the immature dengue virus at low pH primes proteolytic maturation. Science. 2008; 319:1834–1837. [PubMed: 18369148]
13. Rodenhuis-Zybert IA, et al. Immature dengue virus: a veiled pathogen? PLoS Pathog. 2010; 6:e1000718. [PubMed: 20062797]
14. Colpitts TM, Rodenhuis-Zybert I, Moesker B, Wang P, Fikrig E, Smit JM. prM-antibody renders immature West Nile virus infectious *in vivo*. J. Gen. Virol. 2011; 92:2281–2285. [PubMed: 21697345]

15. Li L, et al. The flavivirus precursor membrane-envelope protein complex: structure and maturation. Science. 2008; 319:1830–1834. [PubMed: 18369147]
16. Kostyuchenko VA, Zhang Q, Tan JL, Ng TS, Lok SM. Immature and mature dengue serotype 1 virus structures provide insight into the maturation process. J. Virol. 2013; 87:7700–7707. [PubMed: 23637416]
17. Ma L, Jones CT, Groesch TD, Kuhn RJ, Post CB. Solution structure of dengue virus capsid protein reveals another fold. Proc. Natl. Acad. Sci. U.S.A. 2004; 101:3414–3419. [PubMed: 14993605]
18. Dokland T, Walsh M, Mackenzie JM, Khromykh AA, Ee KH, Wang S. West Nile virus core protein; tetramer structure and ribbon formation. Structure. 2004; 12:1157–1163. [PubMed: 15242592]
19. Wang L, et al. From mosquitos to humans: Genetic evolution of Zika virus. Cell host & microbe. 2016; 19:561–565. [PubMed: 27091703]
20. Pierson TC, et al. The stoichiometry of antibody-mediated neutralization and enhancement of West Nile virus infection. Cell Host Microbe. 2007; 1:135–145. [PubMed: 18005691]
21. Nelson S, et al. Maturation of West Nile virus modulates sensitivity to antibody-mediated neutralization. PLoS Pathog. 2008; 4:e1000060. [PubMed: 18464894]
22. Davenport TM, et al. Isolate-specific differences in the conformational dynamics and antigenicity of HIV-1 gp120. J. Virol. 2013; 87:10855–10873. [PubMed: 23903848]
23. Kwong PD, et al. HIV-1 evades antibody-mediated neutralization through conformational masking of receptor-binding sites. Nature. 2002; 420:678–682. [PubMed: 12478295]
24. Dejnirattisai W, et al. Dengue virus sero-cross-reactivity drives antibody-dependent enhancement of infection with zika virus. Nat. Immunol. 2016; 17:1102–1108. [PubMed: 27339099]
25. Tirado SM, Yoon KJ. Antibody-dependent enhancement of virus infection and disease. Viral Immunol. 2003; 16:69–86. [PubMed: 12725690]

METHODS-ONLY REFERENCES

26. Tang G, et al. EMAN2: an extensible image processing suite for electron microscopy. J. Struct. Biol. 2007; 157:38–46. [PubMed: 16859925]
27. Scheres SH. RELION: implementation of a Bayesian approach to cryo-EM structure determination. J. Struct. Biol. 2012; 180:519–530. [PubMed: 23000701]
28. Guo F, Jiang W. Single particle cryo-electron microscopy and 3-D reconstruction of viruses. Methods Mol. Biol. 2014; 1117:401–443. [PubMed: 24357374]
29. Pettersen EF, et al. UCSF Chimera--a visualization system for exploratory research and analysis. J. Comput. Chem. 2004; 25:1605–1612. [PubMed: 15264254]
30. Katoh K, Standley DM. MAFFT multiple sequence alignment software version 7: improvements in performance and usability. Mol. Biol. Evol. 2013; 30:772–780. [PubMed: 23329690]
31. Robert X, Gouet P. Deciphering key features in protein structures with the new ENDscript server. Nucleic Acids Res. 2014; 42:W320–W324. [PubMed: 24753421]
32. Pickett BE, et al. ViPR: an open bioinformatics database and analysis resource for virology research. Nucleic Acids Res. 2012; 40:D593–D598. [PubMed: 22006842]

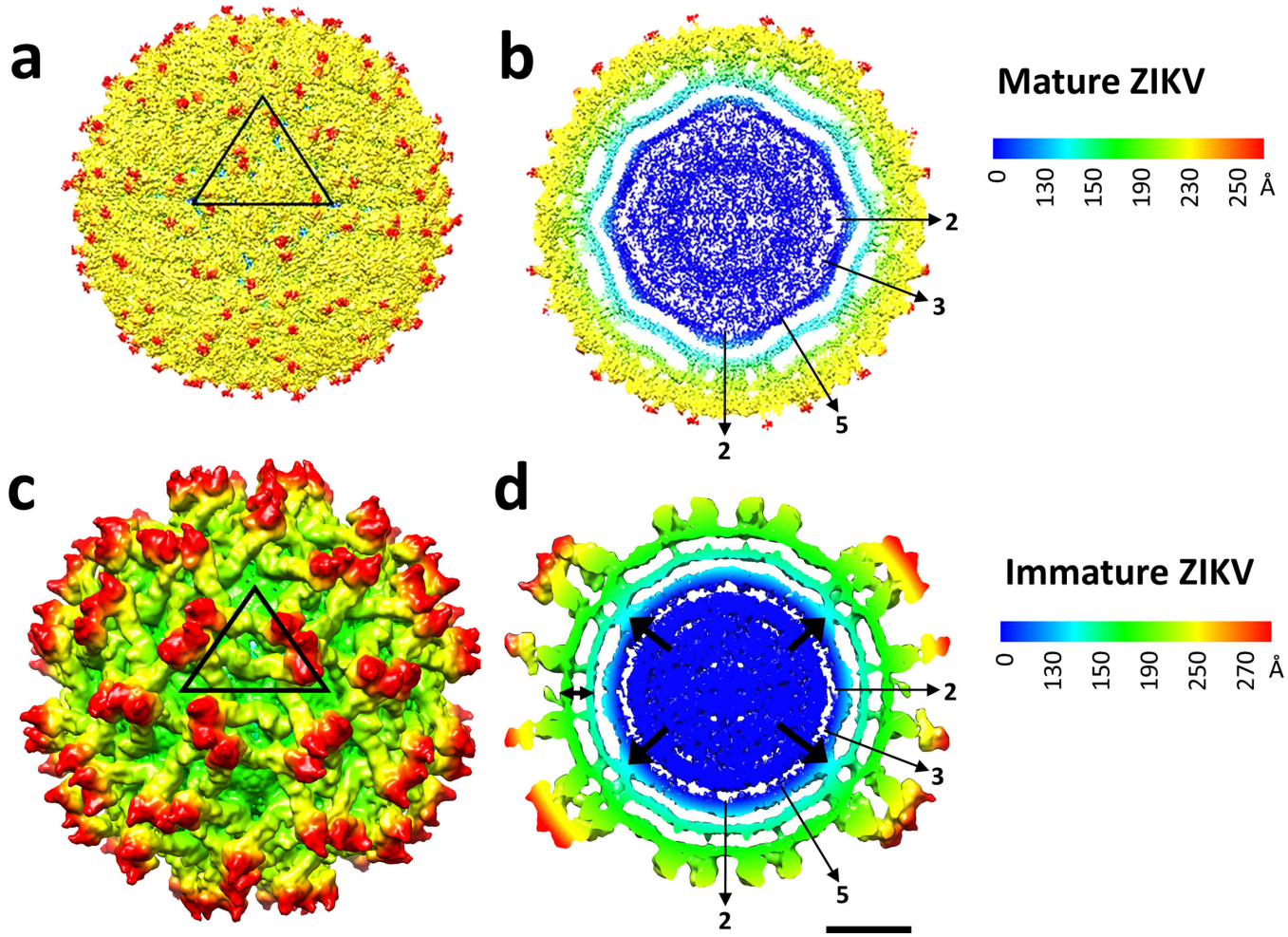

Figure 1.

Cryo-EM structure of immature Zika virus. Surface view (**a** and **c**) and cross-section (**b** and **d**) of mature[8] and immature ZIKV colored radially. Black arrows indicate the density between the inner RNA core and the viral membrane (double-ended arrow shows the inside and outside layers of the membrane) in immature ZIKV. The asymmetric unit is given as a black triangle in panels **a** and **c**. Scale bar is 100 Å long.

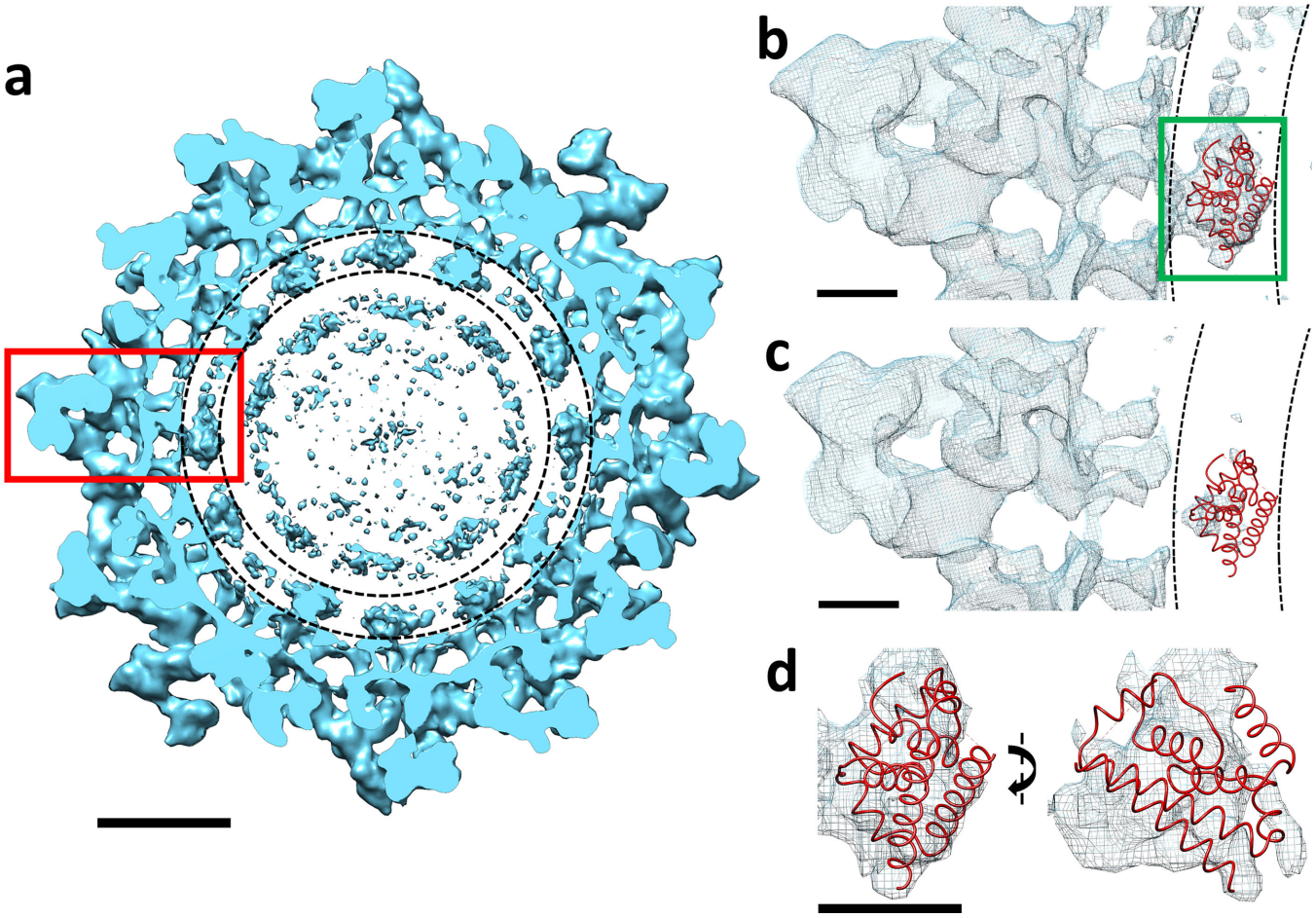

Figure 2.

Cross-section of the immature ZIKV contoured to show the inner capsid shell. (**a**) Cross-section of immature ZIKV projected down an icosahedral 2-fold axis. The putative location of the inner capsid shell lies between the dashed concentric circles. Scale bar is 100 Å in length. (**b** and **c**) Magnified view of the red rectangle region in panel **a** showing the fitted NMR structure of the DENV-2 capsid protein (PDB ID: 1R6R). Panel **b** is rendered at the same contour level as panel **a** whereas panel **c** is rendered at a higher contour level, showing that the capsid protein density height is only about half of that of the outer glycoproteins. (**d**) Magnified view of the dark green rectangle in panel **b** showing the fitted DENV-2 capsid protein structure along two orthogonal views. Scale bar is 25 Å long in panels **b**, **c** and **d**.

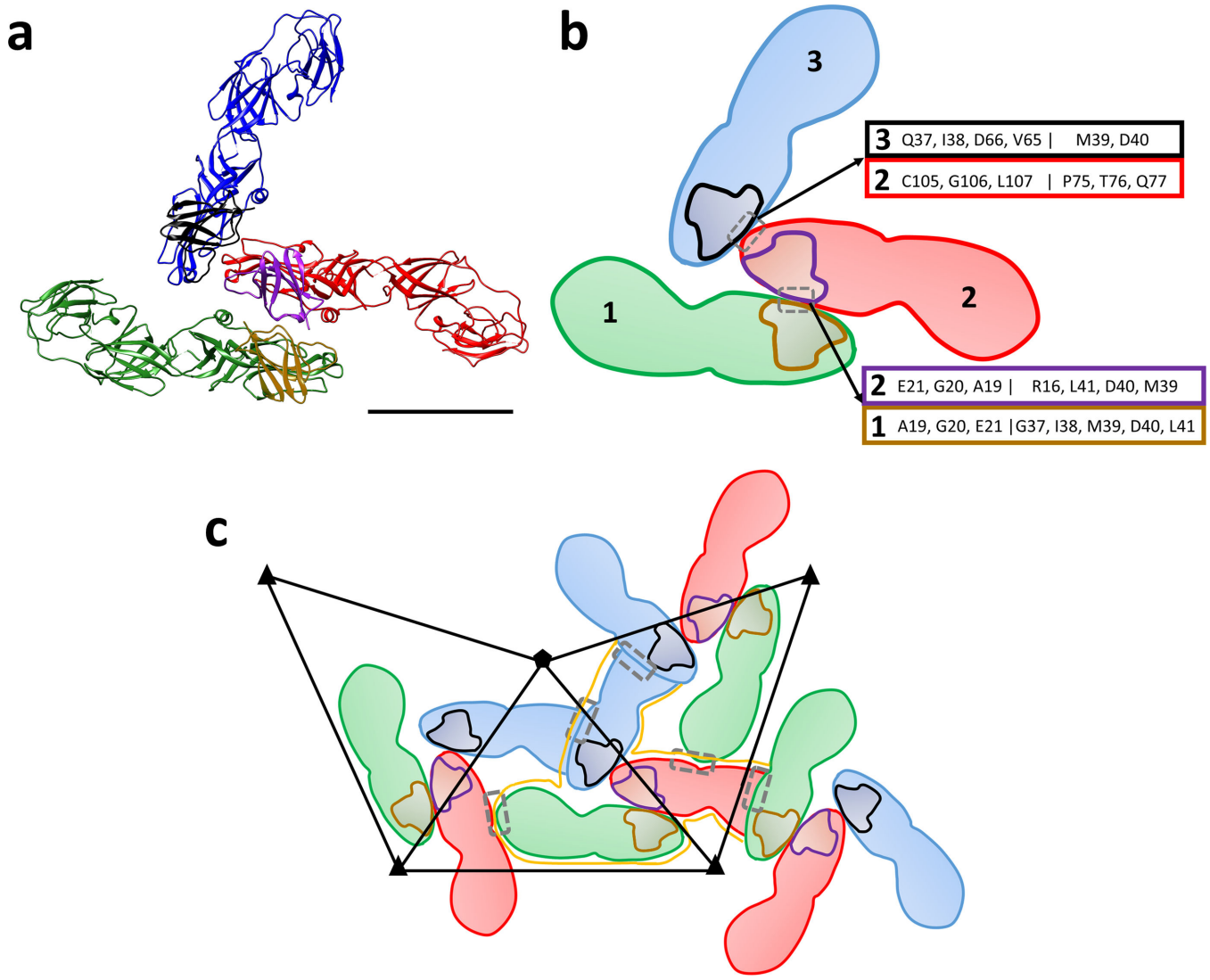

Figure 3.

Interface between prM-E heterodimers. (**a**) Ribbon diagram of prM-E heterodimers in a trimeric spike of immature ZIKV. The prM-E heterodimers are colored in green, red and blue for the E proteins whereas the pr domains are outlined in brown, purple and black, respectively. Scale bar is 50 Å long. (**b**) Diagram of the prM-E arrangement in panel **a** using the same color coding. The three prM-E molecules are marked 1, 2 and 3. The two different interaction regions within trimeric spikes are indicated by a grey box. The molecule number and the residues involved on either side of an interaction surface are given in boxes that are colored according to the protein involved. (**c**) Diagrammatic representation of the trimeric spikes across adjacent asymmetric units. The interaction regions between E proteins from different spikes are indicated as grey rectangles. A single trimeric spike is outlined in orange. The asymmetric unit is outline with a black triangle.